

# A case of spillover rain coinciding with bushfire smoke

Fulong Lu<sup>1</sup> and Chris Webster<sup>1</sup>

<sup>1</sup> Meteorological Service of New Zealand (MetService – Te Ratonga Tiorangi), PO Box 722, Wellington, New Zealand  
Corresponding author: Fulong Lu, fulong.lu@met.service.com

## KEY WORDS

Heavy rain, thunderstorm, lightning, smoke, bushfire, spillover, ice nuclei, forecasting

---

## ABSTRACT

Spillover rain occurs when orographically enhanced rain on the windward side of a mountain range is blown onto the lee side of the range. In Canterbury, this typically occurs in a strong northwesterly airstream ahead of an active front moving up the South Island of New Zealand (NZ). These northwesterly airstreams are of two types: one is a more common situation with a statically stable airmass, and the other involves an unstable airmass.

In general, northwesterly winds bring dry weather to the Canterbury Plains ahead of fronts. In a statically stable northwesterly storm, the rainfall maximum occurs on the windward upper slope of the Southern Alps. In an unstable northwesterly storm, the rainfall maximum shifts to the main divide of the Southern Alps, bringing wet weather ahead of the front in Canterbury. The storm of 6 - 7 December 2019 occurred in a particularly unstable environment (very large Total-Totals and CAPE) with strong upward motion on the West Coast and involved smoke particles from Australian bushfires.

The storm produced a new 24-hour lightning strike record and extensive rain and lightning across the Southern Alps and into South Canterbury, leading to the Rangitata River flooding onto the Canterbury Plains. The mechanism for such lightning to spread east to the Canterbury coast is explored. A secondary rainfall maximum was found on the South Canterbury coast under a quasi-stationary leeward mountain wave. The smoke particles likely played a role in the spillover and lightning. A conceptual model of enhanced spillover rain due to smoke particles in an unstable northwest flow is proposed.

---

## 1. INTRODUCTION

Orographic effects on precipitation have been studied by meteorologists around the world (e.g., Browning et al., 1974; Collier, 1975; Marwitz, 1980; Henderson, 1993; Singh et al., 1995). Several studies into the orographic influences on weather have been made in NZ, especially in the 1990s with the Southern Alps Experiment (e.g., SALPEX, Wratt, et al., 1996). The distribution and spillover of precipitation in the Southern Alps have been explored (Sinclair et al., 1997), including the influence of atmospheric conditions on spillover (Chater, et al., 1998;

Wratt, et al., 2000). Detailed studies of spillover heavy precipitation in the Southern Alps when smoke particles were present have not been carried out.

The Southern Alps run an approximately 500km NE-SW oriented barrier to the predominantly westerly flow over NZ's South Island. Many peaks exceed 2500m in altitude between Westland and Canterbury (Figure 1).

When a cold front moves up the South Island, rain falls in the west ahead of the front, followed by a clearance or partial clearance. In the east, high clouds spread ahead of the front, and rain typically falls behind it in the post-frontal southerly or southwesterly airstream. Near the front, rain

---

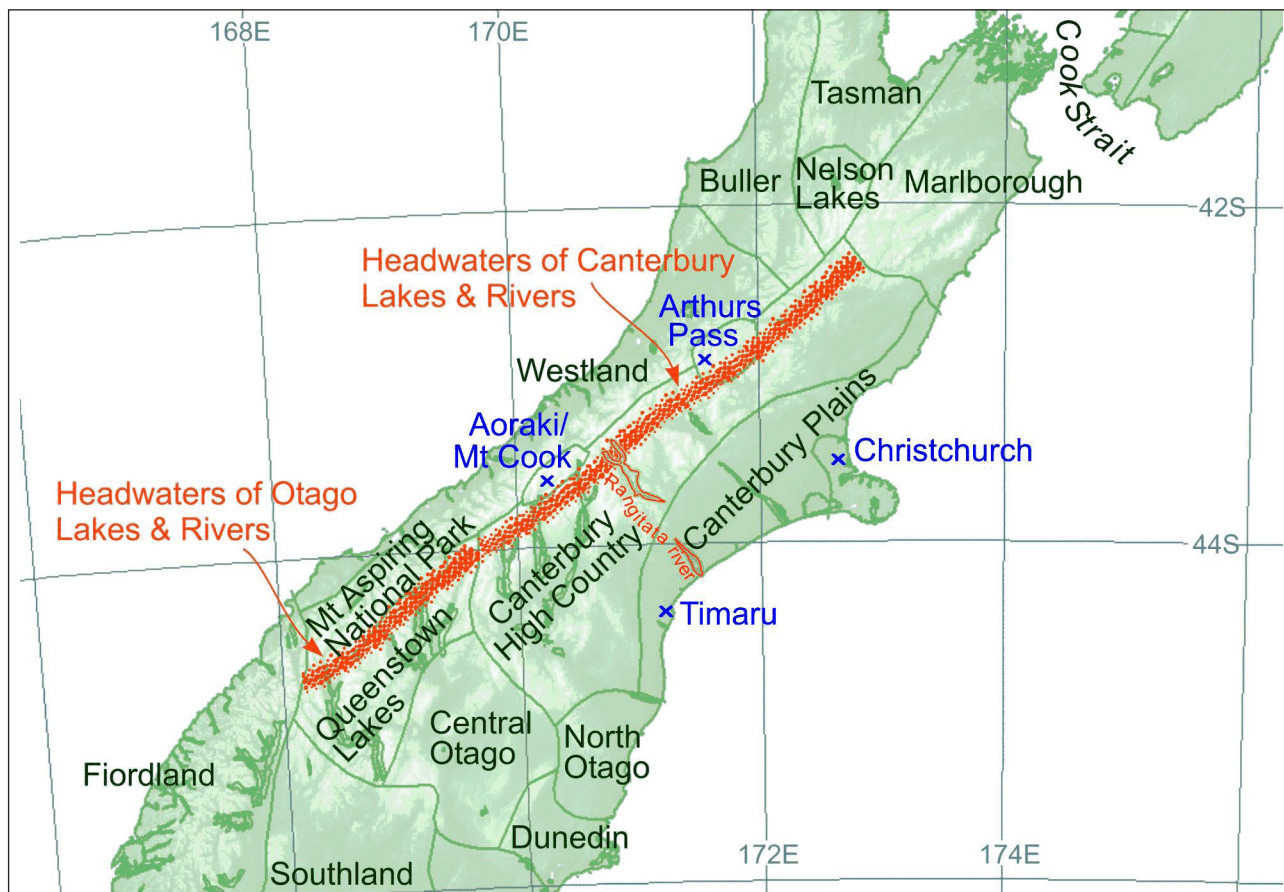


**Figure 1:** Map of the South Island with regional names and simplified topography. Main locations mentioned in the paper are marked, including the headwaters of the Otago and Canterbury lakes and rivers, and the Rangitata River (red).

spills over the headwaters of the Canterbury (and Otago) lakes and rivers, with a rain shadow further east. Figure 2 shows this weather pattern when the pre-frontal airmass is statically stable.

The extent of spillover heavy rain depends on:

1. the static stability of the pre-frontal airmass,
2. the baroclinicity of the front,
3. the amount of moisture advected in from upstream,
4. the vertical wind profile west of the mountains (both speed and direction),
5. the amount of upper-level divergence, and
6. the speed of movement of the front.

Further to point 1, in unstable northwesterly airstreams, rain ahead of the front spreads more readily across the Southern Alps onto the Canterbury Plains.

Many extreme weather events (EWEs) in NZ are associated with atmospheric rivers (ARs) (Reid et al., 2021; Little et al., 2019; Kingston et al., 2016), however, little is known about the effect of smoke particle ingestion on EWEs. The case study presented in this paper involves bushfire smoke particles. The aim is to better understand

smoke particles' effect on atmospheric instability and cloud physics, and how that could enhance spillover heavy rain. It is also intended to improve the forecasting of EWEs.

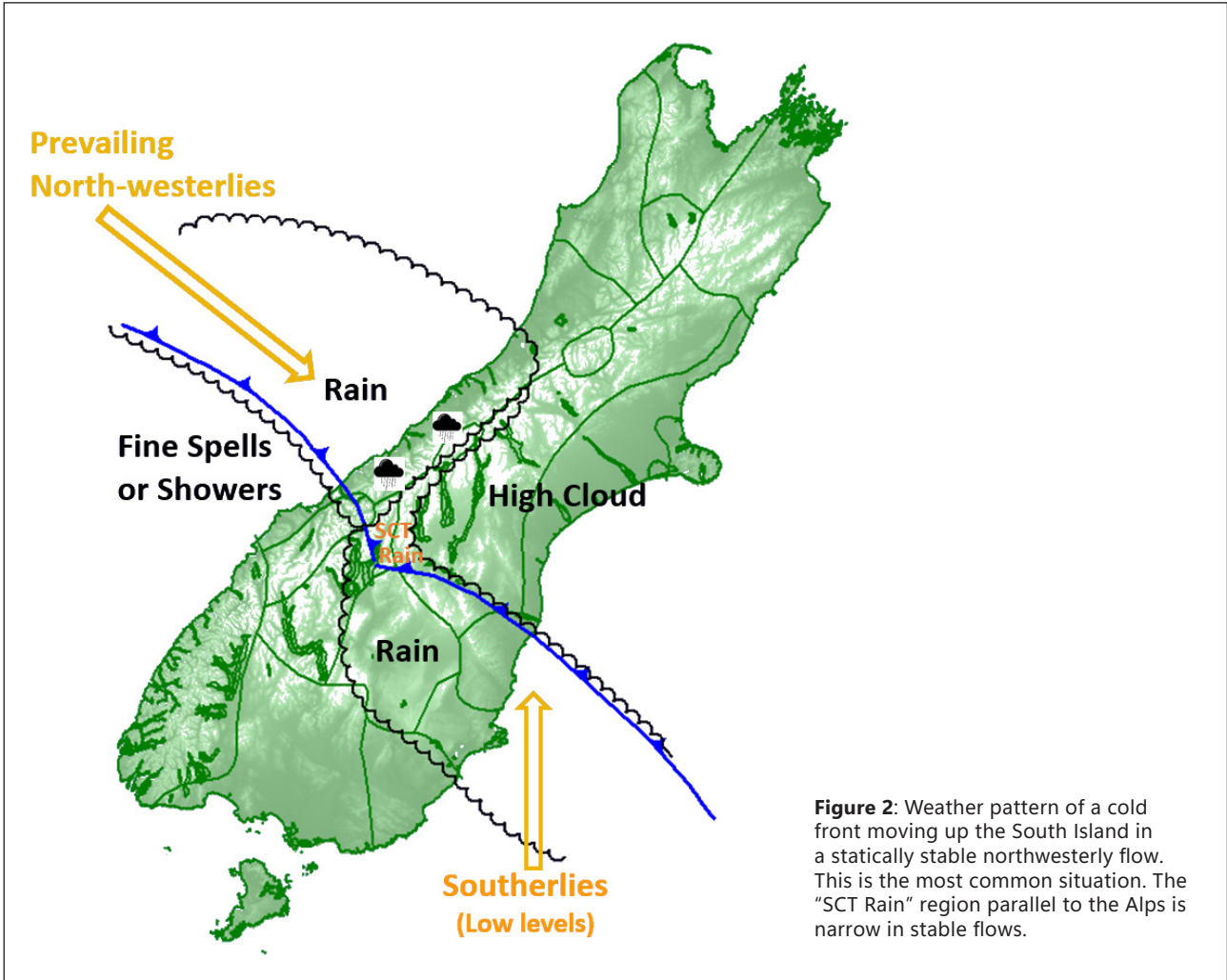
## 2. DATA SOURCES

### 2.1 Rainfall observations and satellite

Rainfall data used in this paper are from NZ MetService real-time hourly data and NZ Regional Council rainfall data. Visible, infrared and water vapour satellite imagery are from the Himawari-8 geostationary satellite of the Japan Meteorological Agency (JMA), except for Figure 6 from the Terra MODIS Corrected Reflectance (True Colour) data supplied by NASA.

### 2.2 Radar

The NZ MetService weather radar network is comprised of ten C-band radars. Data from two of these radars, Westland and Canterbury, are used in this study. These two



radars are on opposite sides of the Southern Alps and are 140km apart. The Westland radar is a Vaisala WRM200 dual polarisation C-band Doppler radar. It is located 8km east of Hokitika at a height of 350m above Mean Sea Level (MSL). The Canterbury radar is an older Ericsson single polarisation C-band Doppler radar, located near Rakaia on the Canterbury Plains at a height of 124m above MSL. Both radars produce three-dimensional scans out to 250 km range every 7.5 minutes. The scans contain 13 elevation angles from 0.5° to 20.0°, with a range bin spacing of 200m at Westland and 125m at Canterbury.

### 2.3 Lightning

Lightning data come from the NZ Lightning Detection Network (LDN). The LDN consists of 10 Vaisala LS7002 sensors, of which 5 are located in the North Island and 5 in the South Island. The network is a hybrid system that uses both Time of Arrival and Magnetic Direction Finding to

locate and classify lightning. The detection Efficiency of the network is modelled to be 95% for Cloud-to-Ground and 50% for Cloud-to-Cloud (including IntraCloud). For the majority of mainland NZ, the Location Accuracy of each flash is within 1km with a 50% confidence interval.

### 3. EVENT DESCRIPTION AND ANALYSIS

In early December of 2019, a week-long period of heavy rain affected the South Island (NZ Historic Weather Events Catalogue, NIWA). Rain fell over the Canterbury headwaters from 1 to 4 December, which pre-conditioned the Rangitata River to flood. There was considerable instability in the Tasman Sea and NZ region.

The storm of 6 to 7 December was the climax of the prolonged event. This coincided with widespread bushfires over eastern Australia from which significant amounts of smoke were blown across the Tasman Sea onto NZ. 101,202 lightning strikes were recorded from 0000UTC



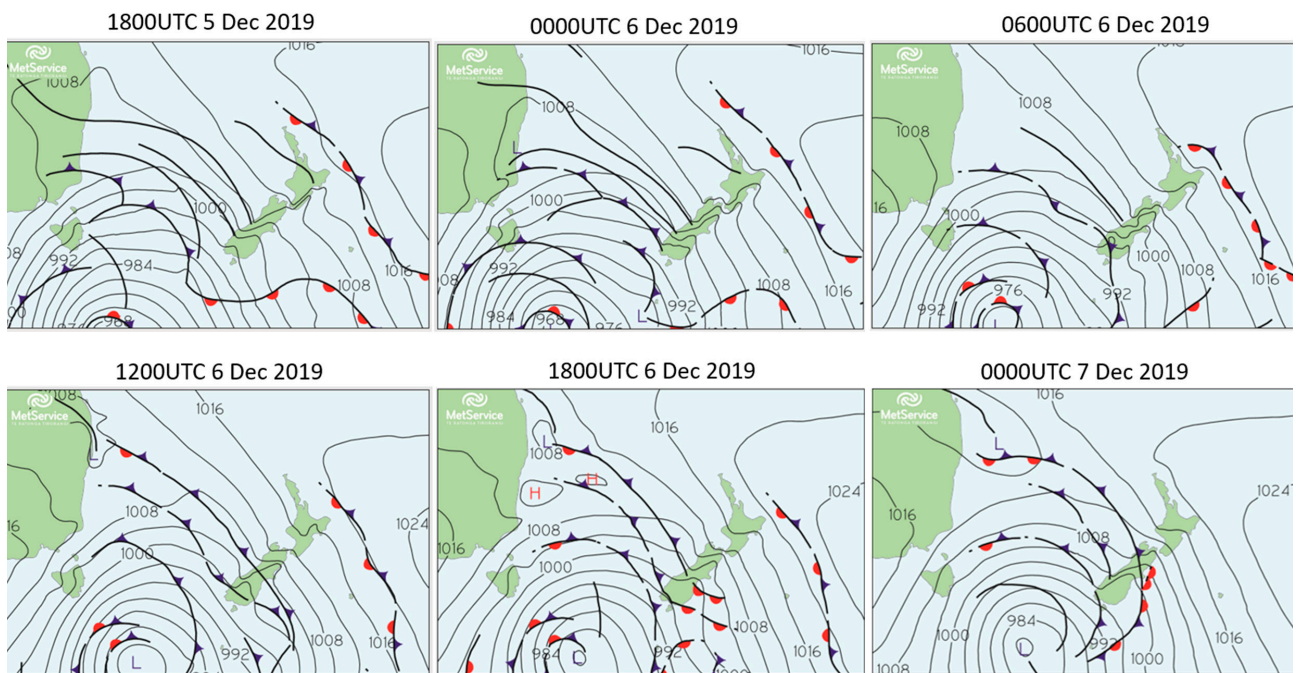
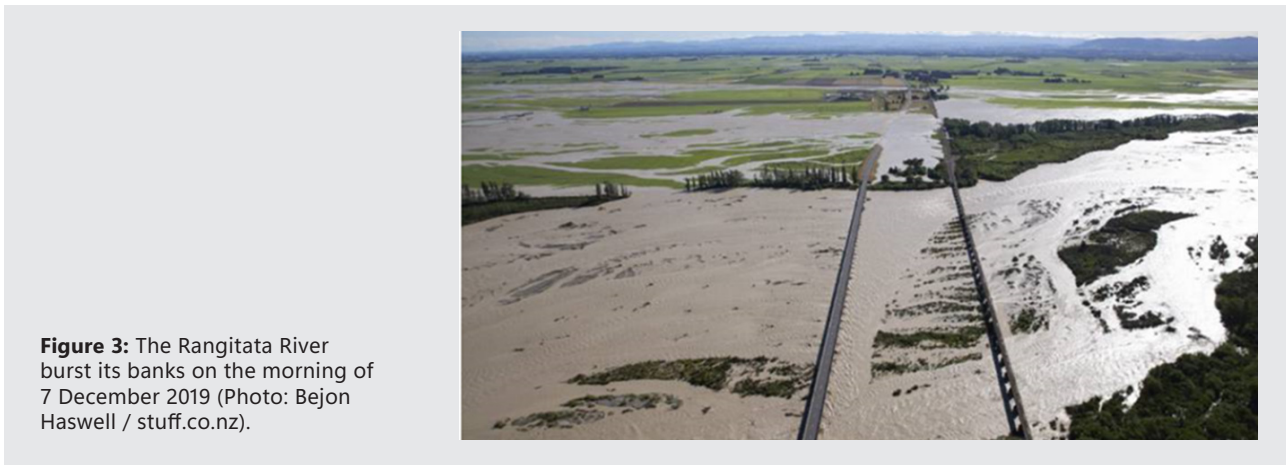
6 to 0000UTC 7 December, which was twice the previous 24-hour record number of strikes (10 April 2018, based on the NZ lightning strike data since 2001). In Westland, 200 to 350mm of rain fell in 24 hours on the ranges but much less near the coast. Heavy rain led to landslides and flooding on the West Coast, cutting off towns and trapping about 1000 tourists. In Canterbury, 200 to 350mm of rain fell in 24 hours about the headwaters of the Canterbury rivers and lakes within 30km east of the main divide of the Southern Alps while, further east, significant but lesser falls were recorded. As context, warnings are issued when more than 50mm of rain in 6 hours or 100mm in 24 hours is expected over a wide area. In the Timaru District, a State of Emergency was declared on the morning of 7 December

after the Rangitata River burst its banks downstream (Figure 3), and the only two bridges north to Christchurch were closed due to flooding.

On 8 December, thunderstorms and heavy rain battered the lower North Island. Nationwide, the storm cost insurers \$15.29M but no deaths were reported.

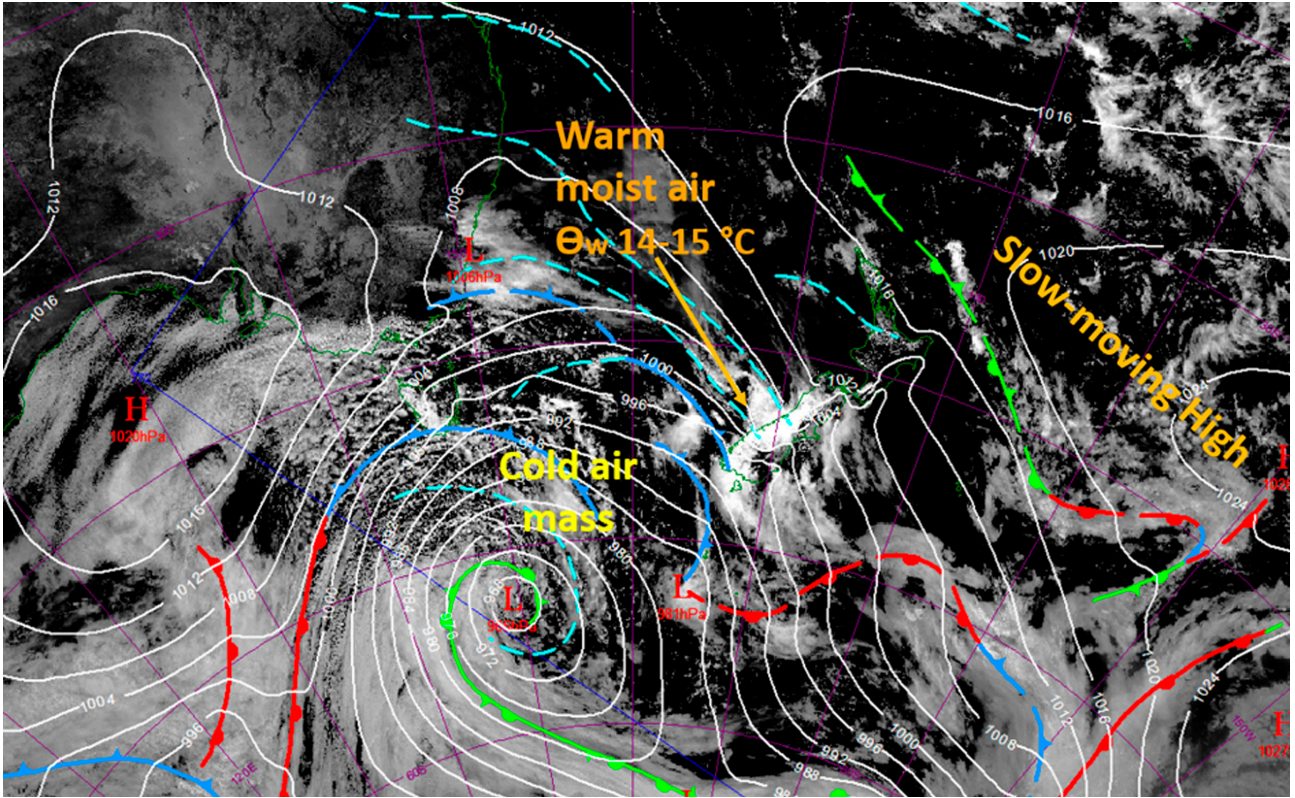
Mean Sea Level Pressure (MSLP) map analyses (Figure 4) indicate a deep low to the south of the Tasman Sea, which brought troughs and fronts onto the South Island. The flow was cyclonic over the Tasman Sea and South Island. The troughs and fronts became slow-moving over the South Island due to a nearly stationary ridge of high pressure to the northeast of NZ.

Figure 5 shows the meteorological set-up, including the



**Figure 4:** MSLP analyses from 1800UTC 5 December to 0000UTC 7 December 2019.





**Figure 5:** MSLP analysis superimposed on visible satellite image at 0000UTC 6 December 2019. Image courtesy JMA.

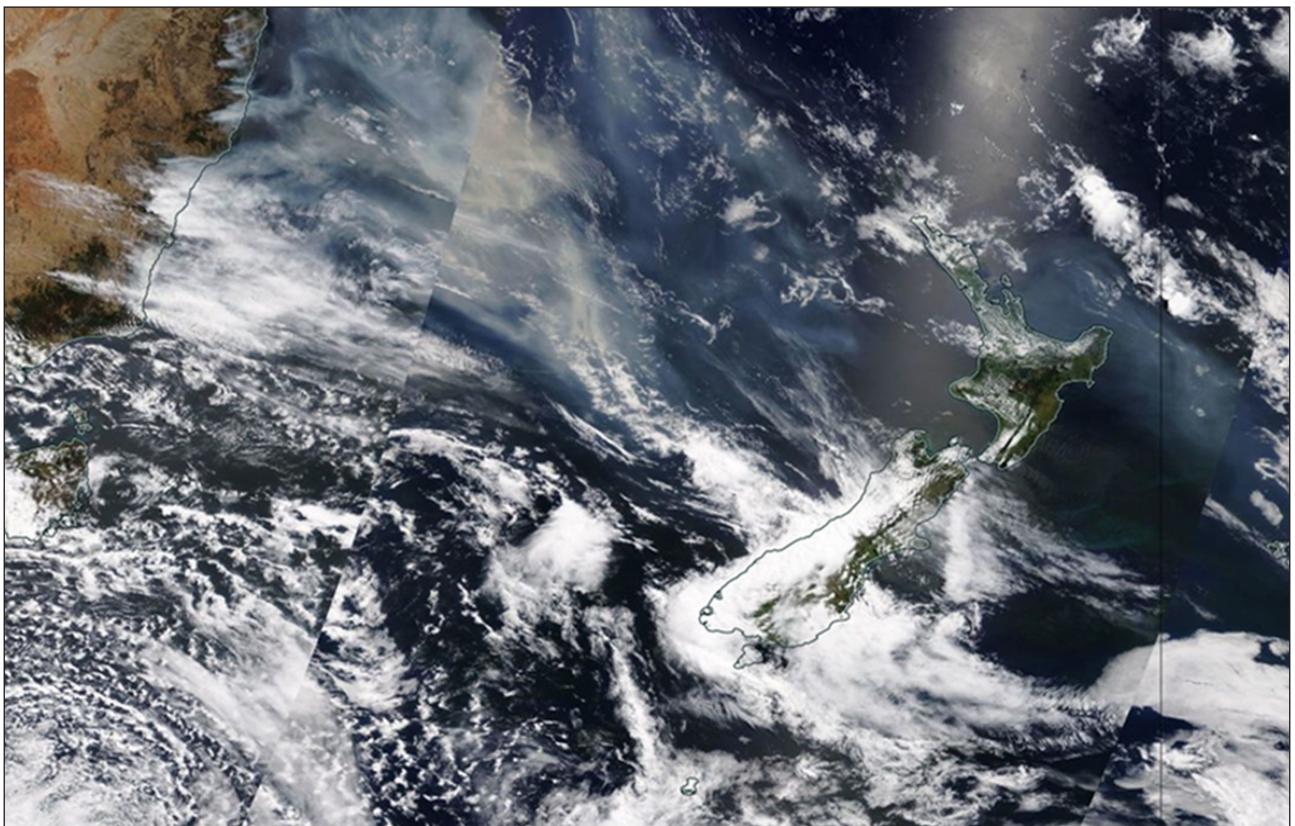
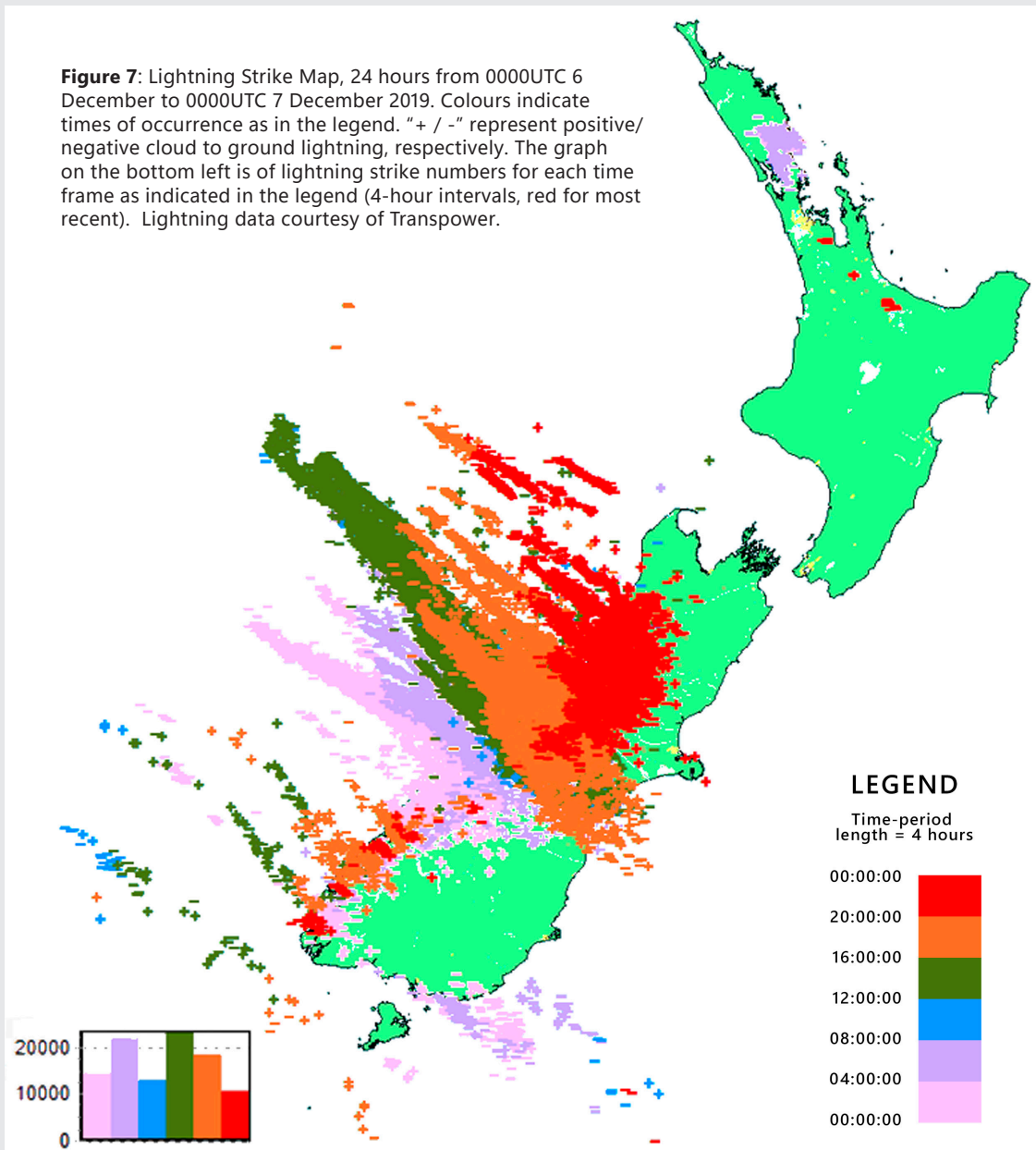


**Figure 6:** Terra MODIS Corrected Reflectance (True Colour) image at 2250UTC 5 December 2019 showing bushfires over eastern Australia with smoke particles (brown) extending over the Tasman Sea near and north of a front on the South Island West Coast. Note, a bright area to the north of the North Island was sun-glint. Image courtesy NASA.

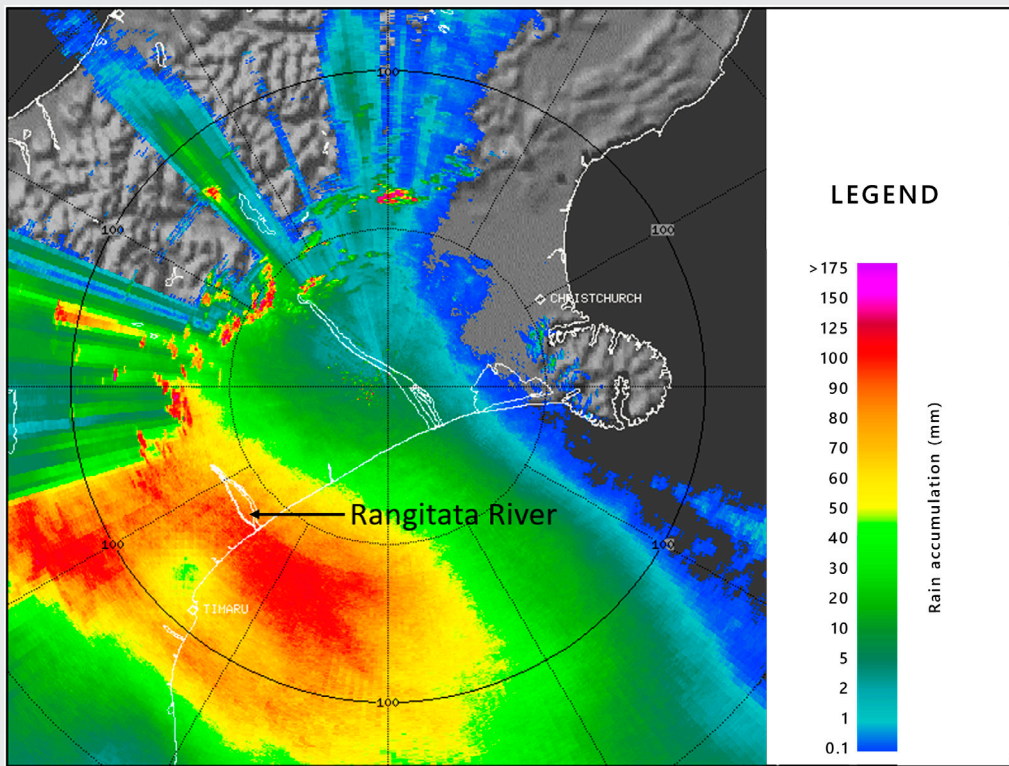
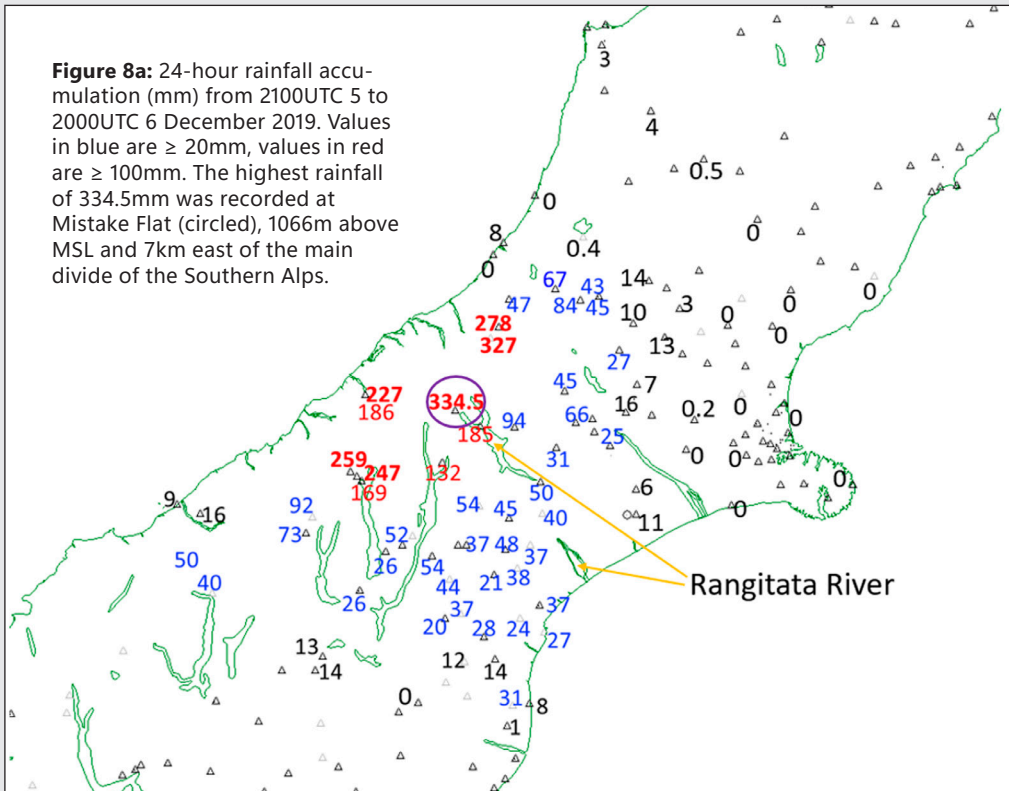
moist northwesterly airstream extending from Australia onto NZ. Rain over the South Island was supported by an upper-level jet and bands of cyclonic vorticity advection at the 500hPa level (not shown), and cold advection from the south Tasman Sea. Figure 6 shows smoke particles from eastern Australian bushfires being blown across the Tasman Sea and becoming caught up in the fronts and troughs over NZ.

The lightning data in Figure 7 indicate a significant number of lightning strikes spread southeast to the

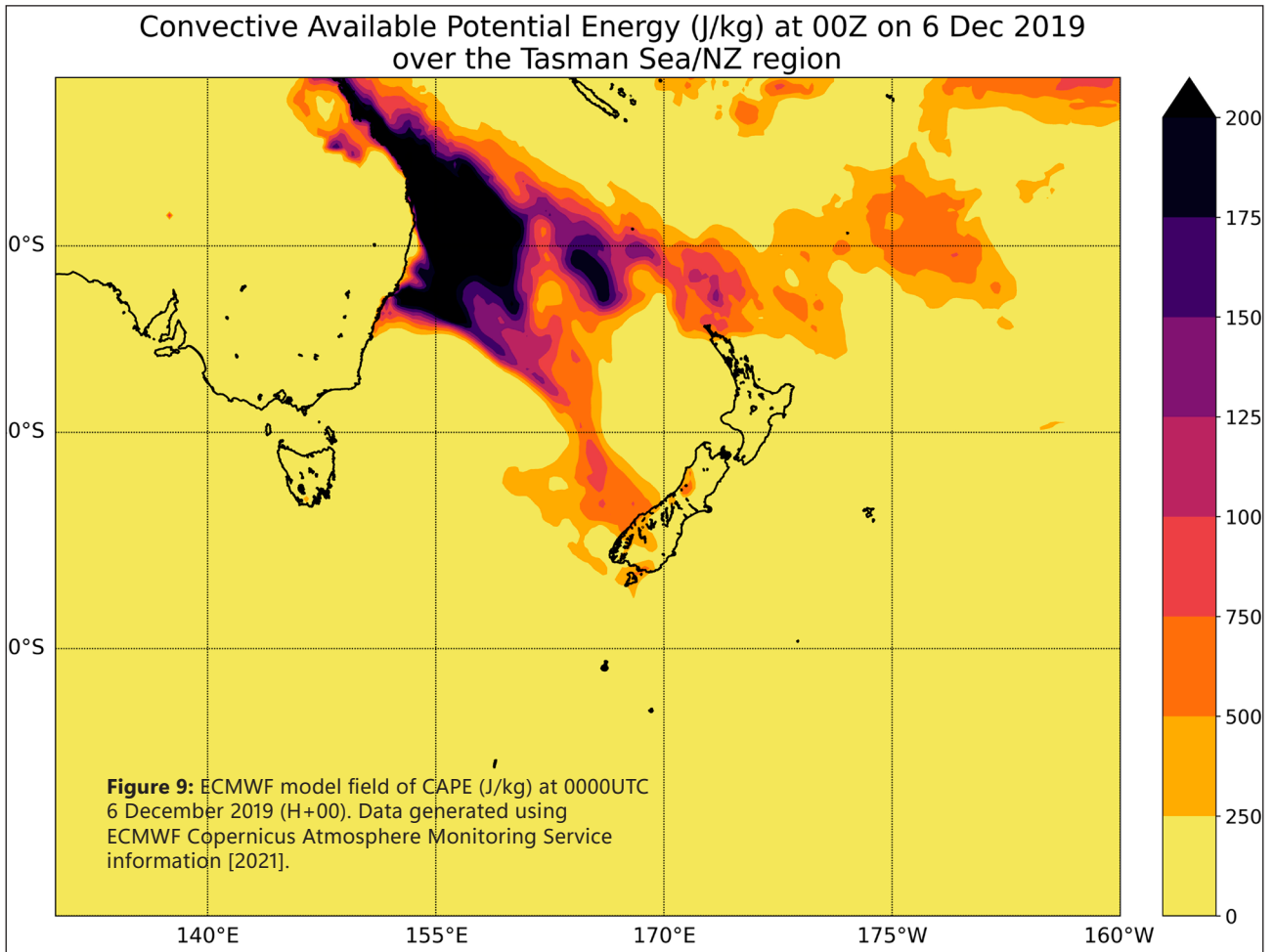
Canterbury coast. Frequent lightning lasted for over 12 hours (0500-1900UTC 6 December) in South Canterbury where an eyewitness confirmed that he “had never seen this in the last 30 years” (personal communication: Laurence Smith, Environment Canterbury, 10/12/2019). The 24-hour rainfall accumulation plot (Figure 8a), valid to 9am 7 December, shows heavy rain spread east to the Canterbury High Country. The heaviest falls occurred about the headwaters of the Rangitata River, and significant rain fell further east into South Canterbury (Figure 8b).











## 4. FINDINGS AND DISCUSSION

### 4.1 Event diagnosis

Modelled Convective Available Potential Energy (CAPE) in Figure 9 indicates substantial instability over the Tasman Sea. Significant CAPE (500-750J/kg) and Normalised Total-Totals<sup>1</sup> (NTT, 52.5-60) on the west of the South Island ahead of the front indicated that static instability was an important factor in generating the active lightning. Precipitable Water Vapour (PWV) was 25-30mm on 6 December and increased to 30-35mm the following morning.

Weather Research and Forecasting (WRF- GFS) model

<sup>1</sup> NTT (Normalised Total-Totals) calibrates the commonly used TT (Total -Totals) atmospheric stability index to correct for airmass dependence. Warm moist atmospheres that are unstable can yield TT values below 50, while cold dry atmospheres with the same overall stability might have values in excess of 60. The NTT normalises all atmospheres such that a value of 50 equates to neutral stability (with values above this indicating deep instability), no matter the location or season (Schwarz, 2004).

tephigrams (Figure 10) confirmed a deep, unstable airmass on the West Coast from the morning of 6 December to the morning of 7 December.

They indicated a buoyant and generally moist (but dry in the middle level at 1200UTC 6 December) airmass ahead of the slow-moving front, and northwesterly winds increasing with height and becoming very strong above mountaintop level. The strong winds favoured the propagation of hydrometeors and convective cells, as the windshear aloft was not so strong as to destroy convection. Winds perpendicular to the Southern Alps increased the orographic enhancement of rain and triggered thunderstorms over the ranges. Figure 10 indicates strong upward motion from low levels up to 300hPa in the hours before the Rangitata River burst its banks. The upward motion was  $-83 \times 10^{-3}$  to  $-220 \times 10^{-3} \text{hPa s}^{-1}$  between 900hPa and 700hPa, and  $-250 \times 10^{-3}$  to  $-330 \times 10^{-3} \text{hPa s}^{-1}$  between 700hPa and 500hPa at 1800UTC 6 December above the central Westland coast. Such values are extremely large for NZ. This set-up drove heavy rain and thunderstorms from the western slopes of the Southern Alps across to east of the Alps.

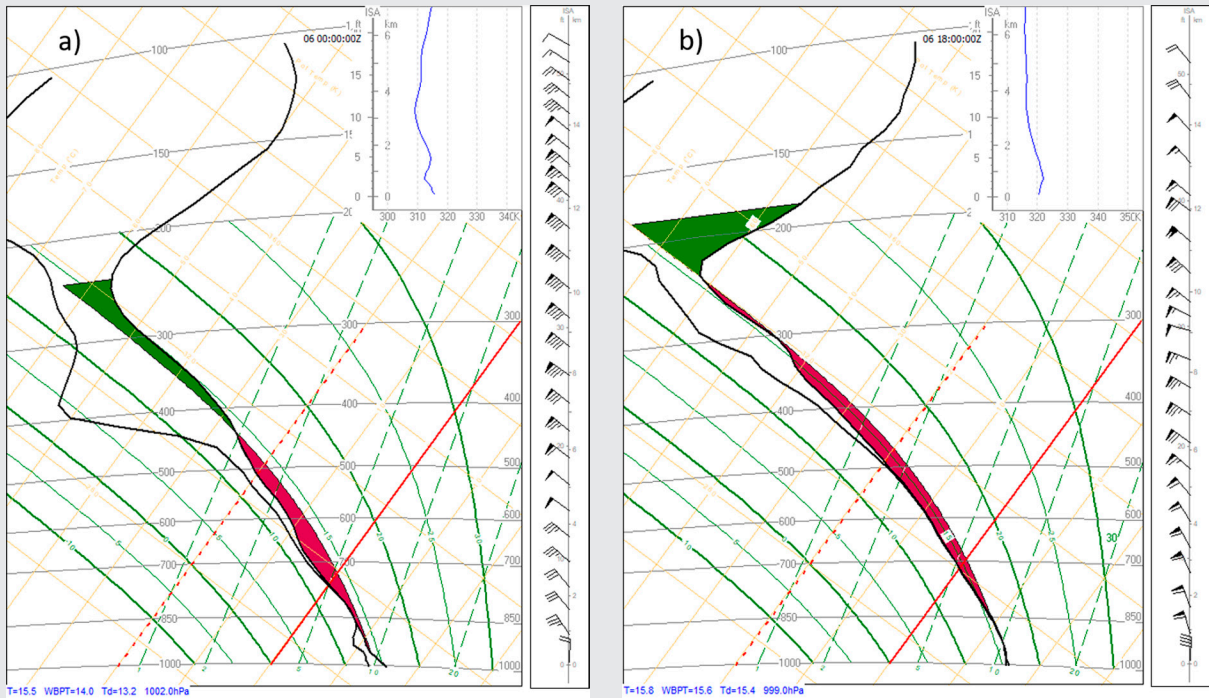


**Figure 10:** NZ4km WRF – GFS model tephigrams (H+00) for the central Westland coast at 0000UTC (left), and 1800UTC (right) 6 December 2019. Yellow lines orientated from top-right to bottom-left are isotherms; yellow lines from top-left to bottom-right are dry adiabats; solid dark-green curves are saturated adiabats. The red shaded area represents CAPE. Wind barbs (right) indicate direction with a full barb =10 knots, half barb = 5 knots, and solid triangle barb =50 knots. Inset at the top right is the equivalent potential temperature (K).

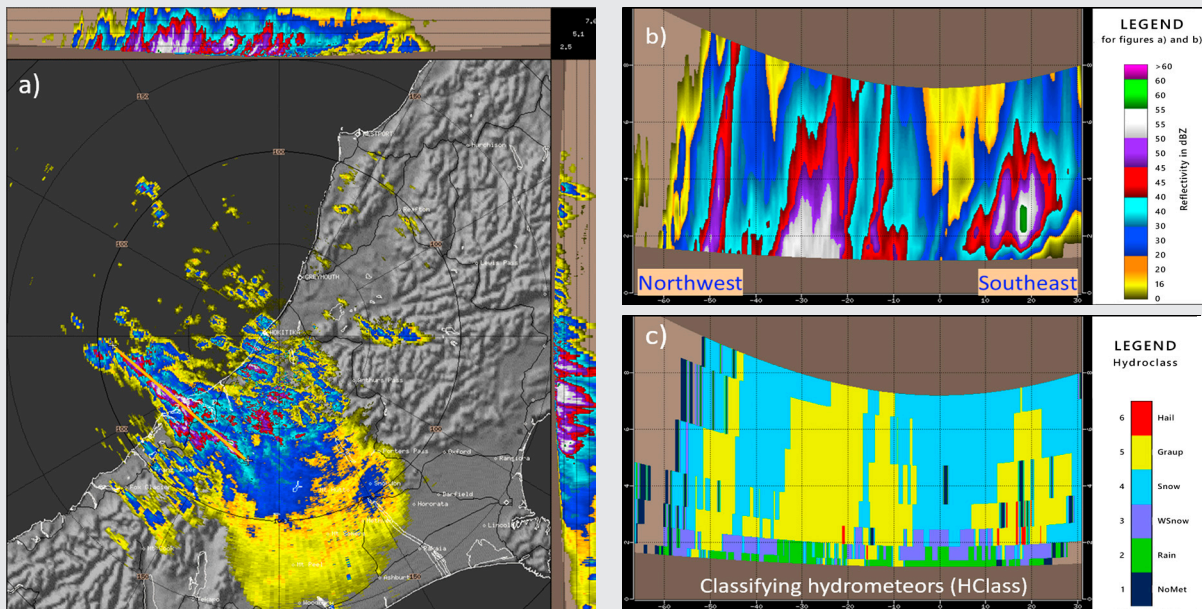


**Figure 11:** a) Westland radar Maximum Reflectivity, b) reflectivity cross-section, and c) HClass cross-section at 12:52UTC 6 December 2019. In a), the main image is maximum reflectivity in the vertical from all available radar beams; top panel is maximum reflectivity from north to south, plotted with respect to height (km); right panel is maximum reflectivity from east to west, also plotted with respect to height (km). The b) and c) cross-sections are taken along the orange line segment in a). Figure b) indicates approximate rainfall intensity: yellow = light precipitation, blue = moderate precipitation, purple/white = heavy precipitation or graupel. Figure c) is the hydrometeor class of b), where green = rain, purple = wet snow, blue = snow, yellow = graupel, red = hail.



## 4.2 Radar signatures

The Maximum Reflectivity composite data of the Westland and Canterbury Radars from 0000UTC to 1800UTC 6 December indicate that strong radar echoes moved onto South Canterbury. Figure 11a shows deep convective cells on the West Coast, tilting eastwards with height due to the wind profile. Figure 11b indicates very strong echoes to mid-high levels. Figure 11c shows extensive graupel (yellow) and some hail (red) within the convective cells. Graupel is being detected at more than 8km above the surface.

Figure 12a shows thunderstorms to the west of the Southern Alps, decaying thunderstorms just east of the main divide, and stratiform precipitation further east. Radar data before and after this time (not shown) indicated similar characteristics.

The inset in Figure 12b is a cross-section from the Canterbury radar along a line from South Canterbury to

snowflakes and/or larger rimed crystals. The cross-section shows enhanced radar reflectivity associated with falling snow about the coast of South Canterbury (ahead of the front). Radar reflectivity time stamps in Figure 13 indicate stronger radar reflectivities (30 - 40dBZ) near the Rangitata River mouth. Tephigrams from WRF (Figure 14) show the upward motion in an upper layer from 380hPa to 200hPa, suggesting the precipitation about the coast of South Canterbury was likely associated with ascent in a quasi-stationary leeward mountain wave (Figure 15).

## 4.3 Eastward spread of thunderstorms and lightning

Aerosols such as smoke particles can enhance lightning activity through modifying cloud microphysical properties and invigorating convection (Yuan et al., 2011; Shi et al., 2020). They can also enhance spillover precipitation in a moist environment through riming and Wegener-Bergeron-Findeisen processes (Choudhury et al., 2019).

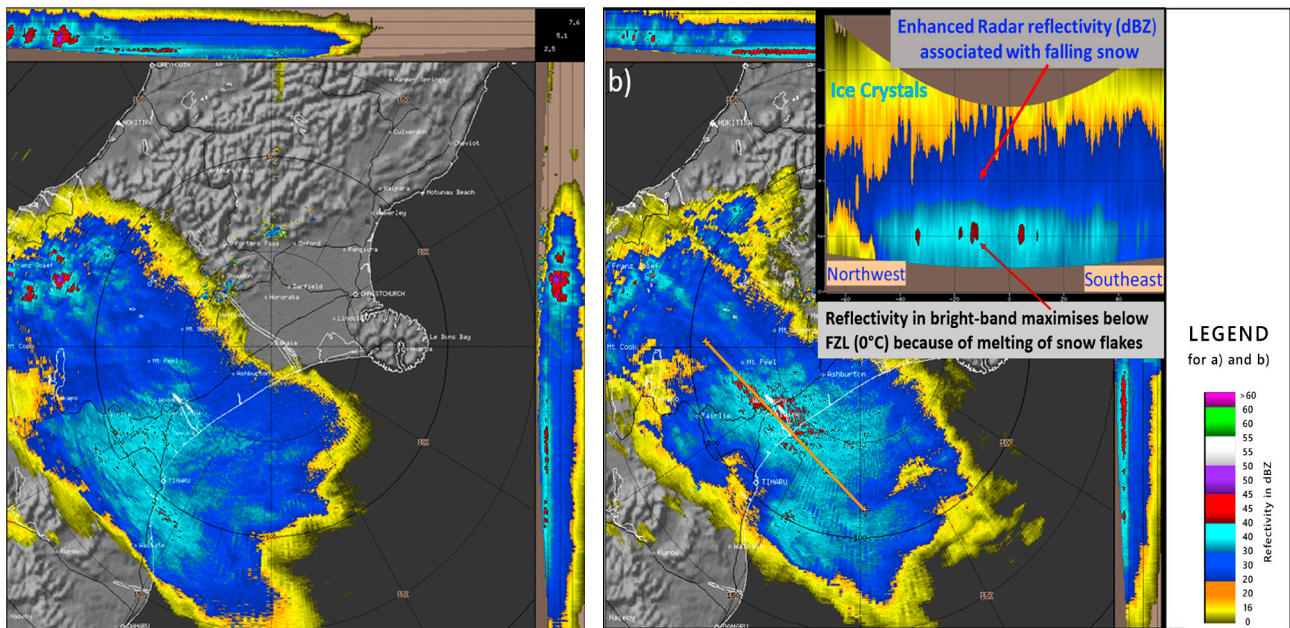


**Figure 12:** **a)** Canterbury radar Maximum Reflectivity at 06:07UTC and **b)** Maximum Reflectivity and cross-section of Canterbury radar (inset) at 07:00UTC 6 December 2019. The cross-section is taken along the orange line segment in the bottom right image. The times were chosen to match the satellite images in Figure 15 b) and c), respectively.

the Canterbury Bight showing enhanced radar reflectivity (dBZ) associated with aggregated or rimed snowflakes in falling snow (the mechanism explained in Figure 14, Ryan et al., 1976), and a radar bright-band associated with rain falling from melting snow below the freezing level. The weaker yellow radar reflectivities are associated with smaller ice crystals blown over the main divide from the west, while the darker blue reflectivities are likely from aggregated

The numerous smoke particles that originated from the Australian bushfires would have provided abundant cloud condensation nuclei (CCN) and ice nuclei, compared to the natural particulate environment dominated by salt CCN in NZ. This would have resulted in the cloud water being distributed into a larger number of smaller ice crystals at high altitudes (likely at the expense of saturated cloud liquid water).



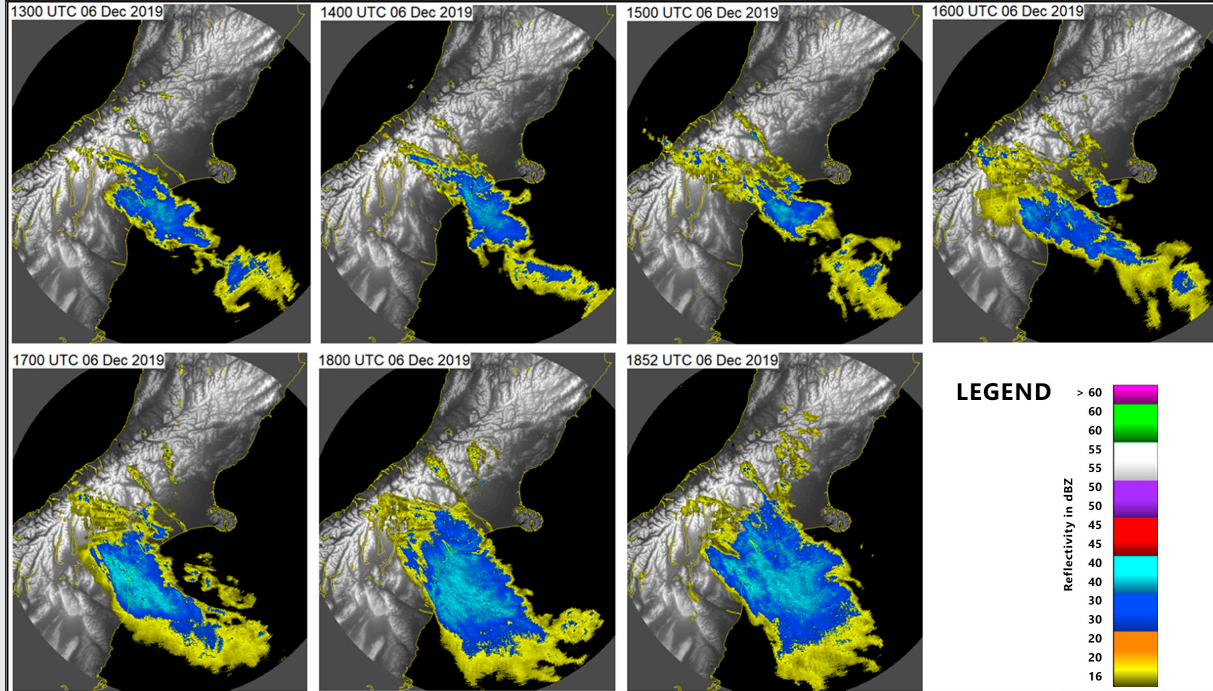
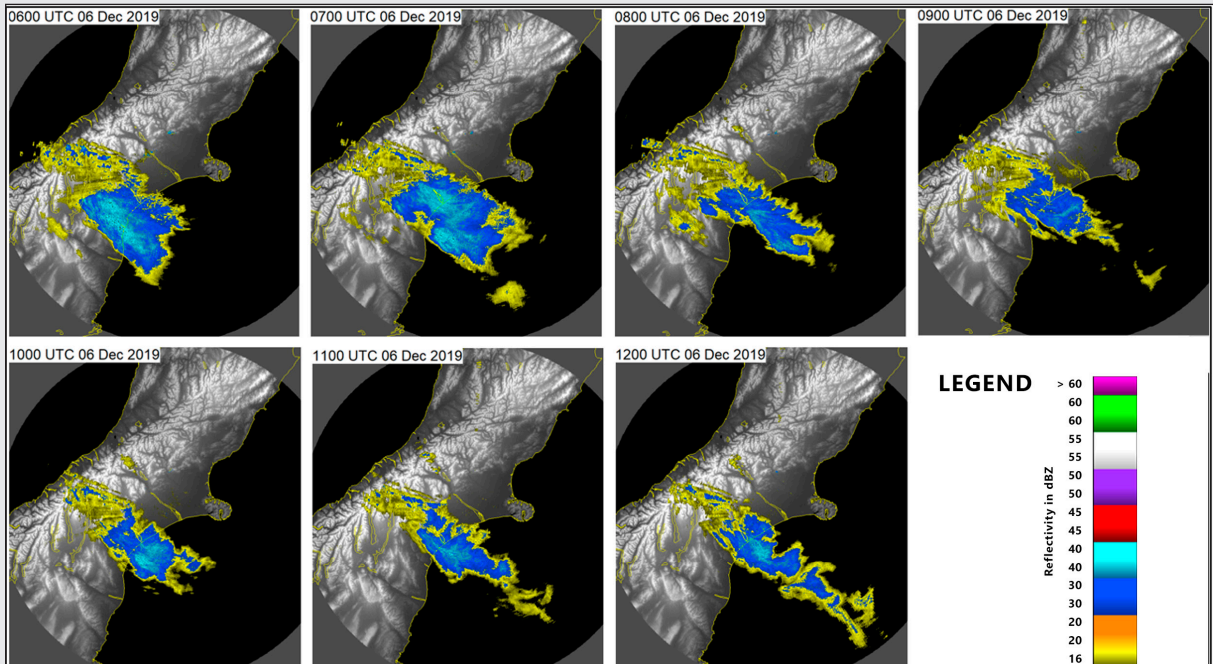


**Figure 13:** Canterbury radar Reflectivity time stamps in dBZ (decluttered, PPI and Elevation 0.5°) top: from 0600UTC to 1200UTC 6 December, bottom: from 1300UTC to 1852UTC 6 December 2019.

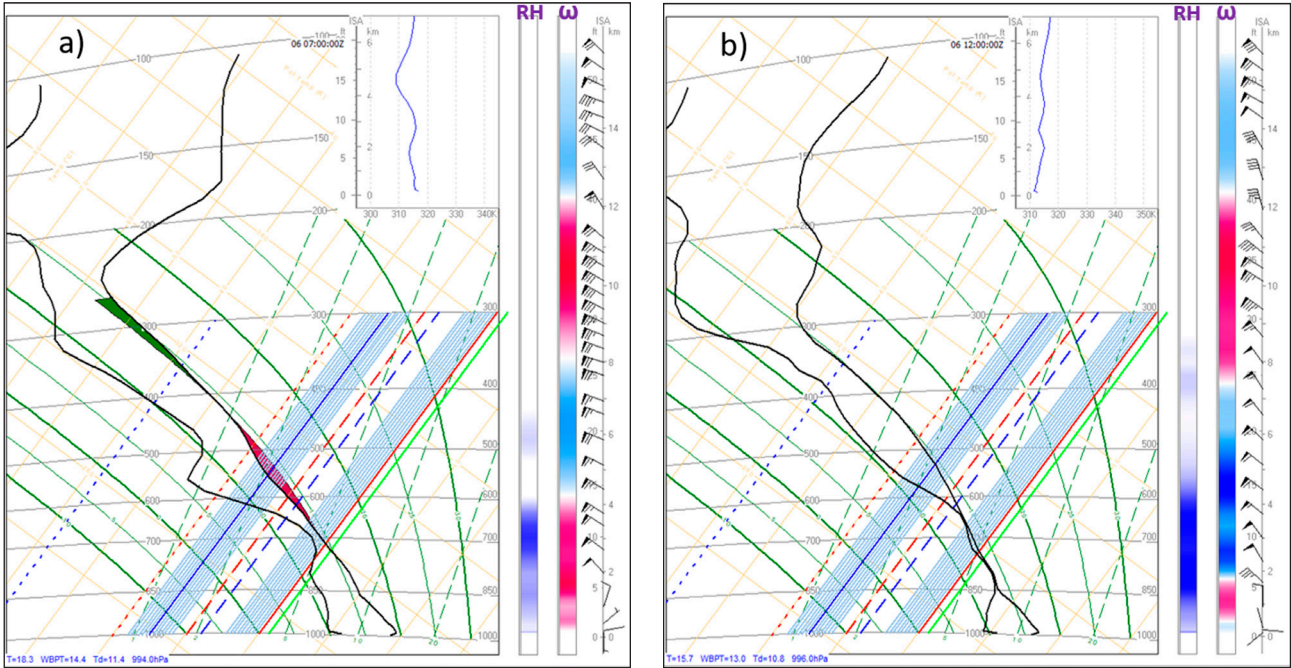


**Figure 14:** NZ4km WRF-GFS model tephigrams for Timaru (near the coast just south of Rangitata River mouth), **a)** 0700UTC 6 December 2019, and **b)** 1200UTC 6 December 2019. See Figure 10 for explanation of key lines on the tephigram. In addition, blue lines orientated from upper-right to bottom-left are snow production temperatures (solid red line is zero-degree line). There are two coloured vertical bars along the y-axis, relative humidity (light blue to dark blue representing RH from 50% to 100%) on the left, and Omega (vertical motion  $\omega$ ) on the right (red representing upward motion and blue representing downward motion). Both a) and b) show that temperature and dewpoint temperature separated when colder than  $-8^{\circ}\text{C}$ ; the airmass was humid between  $-4^{\circ}\text{C}$  and  $0^{\circ}\text{C}$  at 0700UTC 6 December, and was near-saturated in a layer between  $-8^{\circ}\text{C}$  and  $+1^{\circ}\text{C}$  at 1200UTC 6 December 2019. This means ice crystals grew by aggregation and accretion (including riming).

REGION	WESTLAND			CANTERBURY HIGH COUNTRY			CANTERBURY PLAINS (incl. Christchurch)		
NUMBER OF STRIKES PER REGION	20,006			23,272			419		
NUMBER OF STRIKES BY TYPE	CG -	CG +	CC	CG -	CG +	CC	CG -	CG +	CC
	13,085	2,855	4,066	14,510	2,495	6,267	186	128	105
PROPORTION OF STRIKES PER REGION TO TOTAL NUMBER OF STRIKES ACROSS ALL THREE REGIONS (%)	45.8			53.3			0.9		

**Table 1:** 24-hour (0000 - 2359UTC 6 December 2019) lightning strike data in Westland and Canterbury High Country and Canterbury Plains. “CC” means Cloud-to-Cloud (including Intra-Cloud) lightning, “CG -” means negative Cloud to Ground lightning, and “CG +” means positive Cloud to Ground lightning.

Table 1 shows that the number of lightning strikes in the Canterbury High Country was significantly greater than in Westland.

Figure 11c indicated abundant graupel to high levels in convective clouds to the west of the Southern Alps (upstream). The process of graupel (or hail) formation is associated with strong cloud electrification, causing more

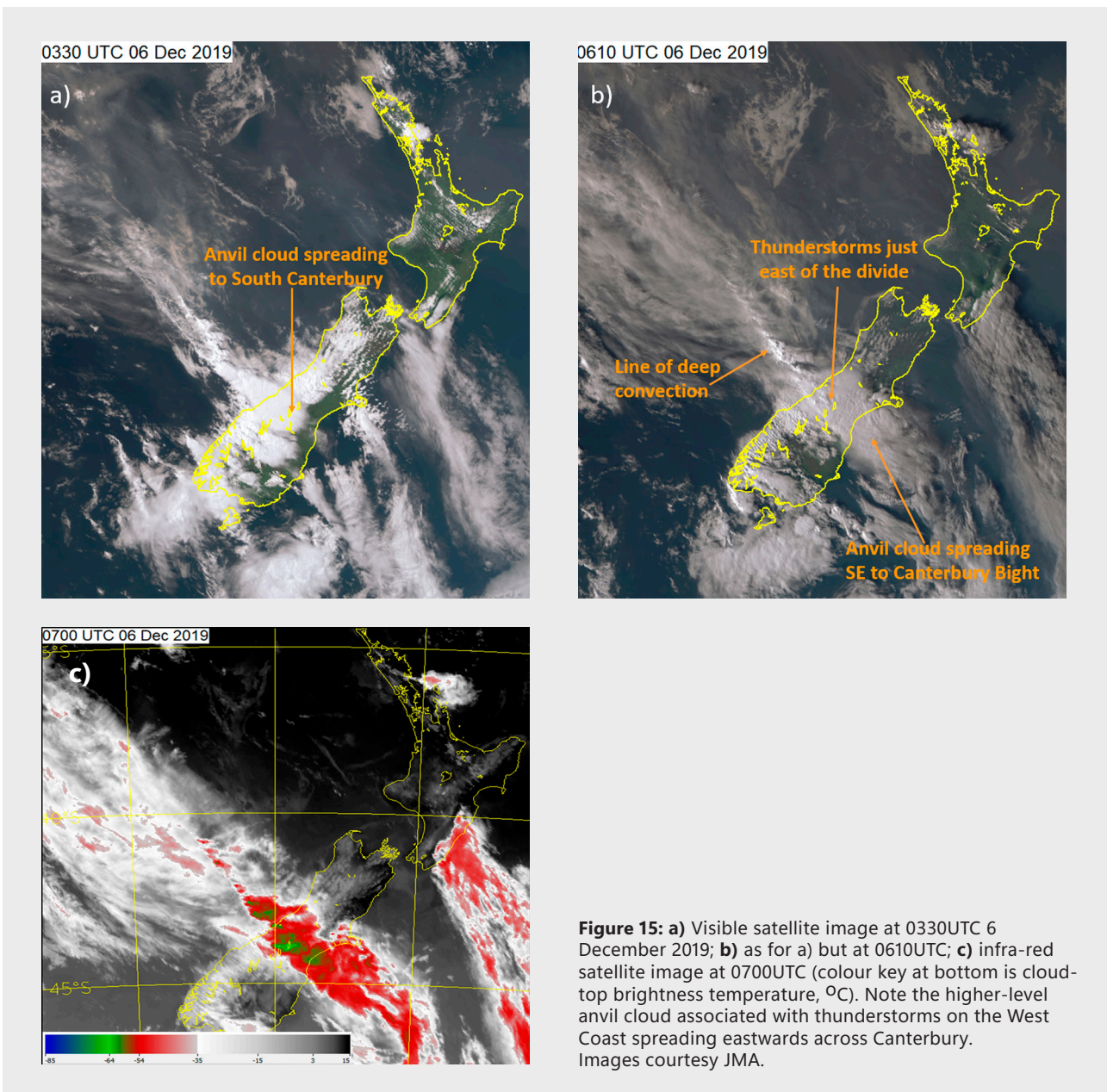
intense thunderstorms (Andreae et al., 2004). Most of the hailstones (graupel) melted as they fell below a high freezing level (2700m), so they arrived at the surface as bursts of heavy rain. This is evident in the radar HydroClass cross-section which (Figure 11c) shows rain (coloured green) as the predominant hydrometeor class at the low levels within the convective cells. Radar imagery (Figure 12a) shows no



convective cells in South Canterbury (not only at this time stamp but also through the 24-hour period), so observed lightning there (from 0500-1900UTC 6 December) was likely due to spillover of charged snow/ice crystals at high altitudes rather than deep convective cells. Strong cross-mountain winds and an unstable airmass (Figure 10) brought abundant charged snow/ice across the Alps onto Canterbury, increasing spillover rain. This process, along with decaying convective cells just east of the main divide, resulted in the maximum rainfall distribution shifting eastward, and warning amounts of rain within 30km east of the main divide. This is consistent with the highest 24-hour rainfall being recorded at Mistake Flat (Figure 8a).

On 6 - 7 December, there was no broad raincloud extending across the Tasman Sea to NZ. However, from the afternoon of 6 December, there was a line of deep convection over the eastern Tasman Sea and Westland, and convective cells that moved across the Southern Alps (Figure 15). An upper “anvil cloud” from cumulonimbus extended towards the Canterbury Bight. The Infrared image (Figure 15c) indicated an area of high cloud tops near the Canterbury coast (green) just to the south of the Rangitata River mouth, coinciding with a secondary rainfall maximum (Figure 8b). This suggests lee-wave enhancement triggered by the Southern Alps.

Lightning was active from 1300UTC to 1900UTC on





6 December when spillover rain was heaviest. Lines of lightning strikes extended from the Tasman Sea onto the West Coast, and the strike density increased on the windward slopes and across the Southern Alps. Lightning then spread southeast to the Canterbury Bight, and most strikes that occurred from the Canterbury foothills to the Bight were Cloud-to-Ground, with one-third positively charged. There was no clear evidence that the wave enhancement increased lightning strikes in South Canterbury.

It is proposed that lightning spread to the Canterbury coast due to the discharge of charged ice crystals from anvil cloud and mid to low-level convective cloud further west, rather than due to deep convection spreading off the Southern Alps. This process lasted for an extended period because the frontal system was slow-moving, the airmass was unstable and the winds across the mountain ridge were strong.

#### 4.4 A conceptual model of enhanced spillover rain with smoke particles in an unstable northwest flow

Figure 16 is a schematic diagram of convective cells about the Southern Alps, spillover rain further east, and significant snow/ice crystals that became electrically charged due to embedded smoke particles. The diagram also shows mountain wave cloud over eastern Canterbury that likely enhanced dendritic growth aloft, resulting in significant rain falling over South Canterbury in a region that would otherwise be dry.

## 5. CONCLUSIONS

The December 2019 storm occurred in a particularly unstable environment and involved smoke particles from Australian bushfires. The airmass had very large NTT (52.5-60) and CAPE (500-750J/kg), and strong upper divergence. The storm was slowed by a nearly stationary high-pressure system to the northeast of NZ. It had strong northwesterlies (but weak windshear) over the Southern Alps, and weak cold advection aloft. Extreme upward motion ( $-250 \times 10^{-3}$  to  $-330 \times 10^{-3} \text{hPa}^{-1}$  between 700 and 500hPa) occurred on the Westland coast ahead of the front.

The storm brought warning amounts of heavy rain to 30km east of the main divide of the Southern Alps, significantly further east than in most EWEs. The maximum 24-hour rainfall shifted to about or just east of the main divide. The storm produced a new 24-hour lightning strike record (101,202) and extensive lightning across the Southern Alps and into South Canterbury. Lightning spreading to the Canterbury coast was likely due to the discharge of charged ice crystals from anvil cloud and mid to low-level convective cloud further west, rather than due to deep convection spreading off the Southern Alps. A secondary rainfall maximum was found on the South Canterbury coast under a quasi-stationary leeward mountain wave.

Smoke particles likely played a role in the spillover and lightning. Without the effect of the smoke particles,

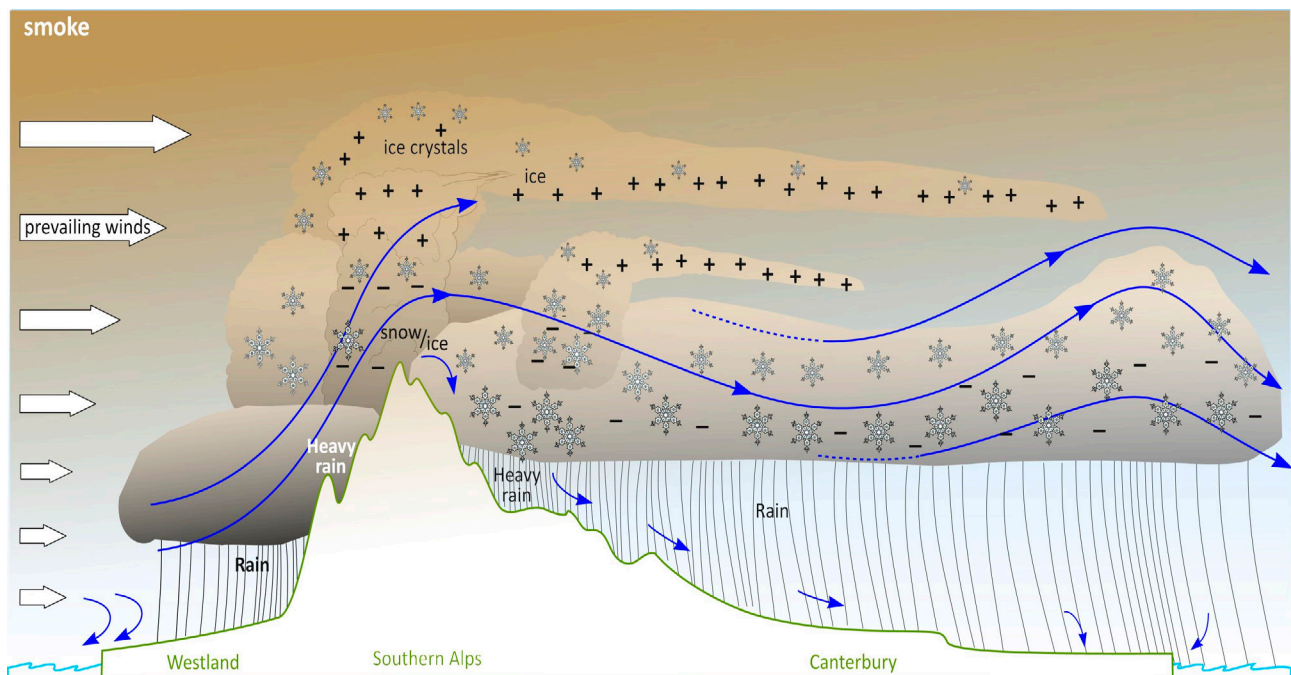


Figure 16: A conceptual model for the 6-7 December 2019 storm.

the number of nuclei would have been much reduced; it is highly likely that thunderstorms to the west of the Southern Alps would have been less active. Rain in South Canterbury ahead of the front would have been lighter and confined to further west. Lightning strikes would similarly have been displaced westwards or much reduced as they spread east across Canterbury.

Due to climate change, spillover heavy rain events could occur more frequently (IPCC, 2022) and may well involve smoke from Australian bushfires. If smoke particles interact with a frontal system, meteorologists should consider the increased potential for heavy spillover rain. This is in terms of both rainfall accumulation and the eastward extent of spillover.

Further research is needed on cases using aerosol concentration data, including the aerosol optical depth (Dayeh et al., 2021; Grell et al., 2011). This should include a mesoscale model coupled with atmospheric chemistry to perform simulations with and without smoke particles in EWEs. This could investigate whether, or under which situations, the smoke particles cause a shift and /or intensification of spillover heavy rain and thunderstorm activity across the Southern Alps of NZ. Other work could look into the effect of varying the number of CCN in mesoscale models and evaluating model performance when smoke particles are present.

## ACKNOWLEDGEMENTS

The authors thank John Crouch, MetService severe weather meteorologist, for his contributions to sections 2.2, 2.3 and 4.2, and Figure 16; Allister Gorman, MetService severe weather meteorologist, for providing lightning strike statistical data; Mark Schwarz, MetService senior consultant meteorologist, for his comments and suggestions, and MetService Forecasting Research and Development team scientists Sijin Zhang for providing information on WRF implementation and Sapna Rana for drafting Figure 9; Leigh Matheson, MetService severe weather meteorologist, for her suggestions; and Chris Knoche, MetService system engineer, for providing lightning data.

## REFERENCES

- Andreae, M.O., Rosenfeld, D., Artaxo, P., Costa, A.A., Frank, G.P., Longo, K.M. and Silva-Dias, M.D., 2004. Smoking rain clouds over the Amazon. *Science*, 303(5662), pp.1337-1342.
- Browning, K.A., Hill, F.F. and Pardoe, C.W., 1974. Structure and mechanism of precipitation and the effect of orography in a wintertime warm sector. *Quarterly Journal of the Royal Meteorological Society*, 100(425), pp.309-330.
- Chater, A.M., Sturman, A.P., 1998. Atmospheric conditions influencing the spillover of rainfall to lee of the Southern Alps, NZ. *International Journal of Climatology: A Journal of the Royal Meteorological Society*, 18(1), pp.77-92.
- Choudhury, G., Tyagi, B., Singh, J., Sarangi, C. and Tripathi, S.N., 2019. Aerosol-orography-precipitation–A critical assessment. *Atmospheric Environment*, 214, p.116831.
- Collier, C.G., 1975. A representation of the effects of topography on surface rainfall within moving baroclinic disturbances. *Quarterly Journal of the Royal Meteorological Society*, 101(429), pp.407-422.
- Dayeh, M.A., Farahat, A., Ismail-Aldayeh, H. and Abuelgasim, A., 2021. Effects of aerosols on lightning activity over the Arabian Peninsula. *Atmospheric Research*, 261, p.105723.
- Grell, G., Freitas, S.R., Stuefer, M. and Fast, J., 2011. Inclusion of biomass burning in WRF-Chem: impact of wildfires on weather forecasts. *Atmospheric Chemistry and Physics*, 11(11), pp.5289-5303.
- Henderson, R.D., 1993. Extreme storm rainfalls in the Southern Alps, New Zealand. *IAHS PUBLICATION*, pp.113-113.
- IPCC, 2022: Climate Change 2022 - *Mitigation of Climate Change: The Intergovernmental Panel on Climate Change*, Skea J., Shukla P. R., Reisinger A., et al., [https://report.ipcc.ch/ar6/wg3/IPCC\\_AR6\\_WGIII\\_Full\\_Report.pdf](https://report.ipcc.ch/ar6/wg3/IPCC_AR6_WGIII_Full_Report.pdf).
- Kingston D.G., Lavers, D.A. and Hannah, D.M., 2016. Floods in the Southern Alps of NZ: the importance of atmospheric rivers. *Hydrological Processes*, 30(26): 5063–5070.
- Little, K., Kingston, D.G., Cullen, N.J. and Gibson, P.B., 2019. The role of atmospheric rivers for extreme ablation and snowfall events in the Southern Alps of NZ. *Geophysical Research Letters*, 46(5), pp.2761-2771.

- Marwitz, J.D., 1980. Winter storms over the San Juan Mountains. Part I: dynamical processes. *Journal of Applied Meteorology and Climatology*, 19(8), pp.913-926.
- NIWA, December 2019 New Zealand Storm. *New Zealand Historic Weather Events Catalogue*. [https://hwe.niwa.co.nz/event/December\\_2019\\_New\\_Zealand\\_Storm](https://hwe.niwa.co.nz/event/December_2019_New_Zealand_Storm).
- Reid, K.J., Rosier, S.M., Harrington, L.J., King, A.D. and Lane, T.P., 2021. Extreme rainfall in NZ and its association with Atmospheric Rivers. *Environmental Research Letters*, 16(4), p.044012.
- Ryan, B.F., Wishart, E.R. and Shaw, D.E., 1976. The growth rates and densities of ice crystals between  $-3^{\circ}\text{C}$  and  $-21^{\circ}\text{C}$ . *Journal of Atmospheric Sciences*, 33(5), pp.842-850.
- Schwarz M., 2004. NTT: Normalising the Total Totals Stability Index, Internal Memo of MetService, NZ (copy available on request to the authors).
- Shi, Z., Wang, H., Tan, Y., Li, L. and Li, C., 2020. Influence of aerosols on lightning activities in central eastern parts of China. *Atmospheric Science Letters*, 21(2), p.e957.
- Sinclair, M.R., Wratt, D.S., Henderson, R.D. and Gray, W.R., 1997. Factors affecting the distribution and spillover of precipitation in the Southern Alps of NZ—A case study. *Journal of Applied Meteorology*, 36(5), pp.428-442.
- Singh, P., Ramasastri, K.S. and Kumar, N., 1995. Topographical influence on precipitation distribution in different ranges of western Himalayas. *Hydrology Research*, 26(4-5), pp.259-284.
- Wratt, D.S., Ridley, R.N., Sinclair, M.R., Larsen, H., Thompson, S.M., Henderson, R., Austin, G.L., Bradley, S.G., Auer, A., Sturman, A.P. and Owens, I., 1996. The NZ southern alps experiment. *Bulletin of the American Meteorological Society*, 77(4), pp.683-692.
- Wratt, D.S., Revell, M.J., Sinclair, M.R., Gray, W.R., Henderson, R.D. and Chater, A.M., 2000. Relationships between air mass properties and mesoscale rainfall in NZ's Southern Alps. *Atmospheric Research*, 52(4), pp.261-282.
- Yuan, T., Remer, L.A., Pickering, K.E., and Yu, H., 2011. Observational evidence of aerosol enhancement of lightning activity and convective invigoration. *Geophysical Research Letters*, 38(4).